Vol. 271: 43–60, 2004 | MARINE ECOLOGY PROGRESS SERIES
Mar Ecol Prog Ser | Published April 28

Combined water-column mixing and benthic boundary-layer flow in mesocosms: key for realistic benthic–pelagic coupling studies

Elka T. Porter[1,*], Lawrence P. Sanford[2], Giselher Gust[3], F. Scott Porter[4]

[1]University of Maryland Center for Environmental Science, Chesapeake Biological Laboratory, 1 Williams Street, Solomons, Maryland 20688, USA

[2]University of Maryland Center for Environmental Science, Horn Point Laboratory, PO Box 775, Cambridge, Maryland 21613, USA

[3]Technische Universität Hamburg-Harburg, Meerestechnik 1, Lämmersieth 72, 22305 Hamburg, Germany

[4]NASA Goddard Space Flight Center, Code 662, Greenbelt, Maryland 20771, USA

ABSTRACT: We developed 2 scaled linked mesocosms that realistically mimicked both water-column mixing and benthic boundary-layer flow, enabling more realistic benthic–pelagic coupling experiments. The first was a 'large' 1000 l system linking a mesocosm with an annular flume; the second a 'small' 100 l system linking a mesocosm with a Gust microcosm. We compared bottom shear velocity, flow speeds, and internal mixing energies between linked and isolated mesocosms that were the same in volume and shape, and compared them to nature. In addition, we performed scaled 4 wk long comparative ecosystem experiments with oysters in the large and small mesocosms to determine if a realistically mimicked benthic boundary-layer flow and system shape could significantly affect ecosystem processes. We scaled all 4 systems to have the same realistic water-column turbulence levels and increased bottom shear velocity to moderate levels in the linked mesocosms. Bottom shear remained unrealistically low compared to nature in the isolated tanks. In addition, the water column and the sediment–water interface were more realistically connected in the linked than in the isolated mesocosms. The linked mesocosms had a similar scaling relationship of turbulence intensity and bottom shear velocity of 1.6, as found in nature. System shape and bottom shear significantly affected ecosystem properties through changes in light, microphytobenthos biomass growth and erosion, sediment inorganic nutrient fluxes, oyster growth, and water column nutrient dynamics. In this study we show that a commonly used system shape in ecosystem studies and unrealistically low bottom shear in mesocosms both produce significant artifacts in benthic–pelagic coupling studies. We also demonstrate improved systems without these artifacts. System shape, bottom shear, water-column turbulence levels, and their ratios should all be considered in designing mesocosms to mimic natural processes.

KEY WORDS: Benthic–pelagic coupling · Flow · Turbulence · Shear velocity · Mesocosm · Experimental ecosystem

INTRODUCTION

In shallow-water environments, 2 goals are to understand the processes that govern benthic–pelagic coupling and to understand how the latter influences ecosystem dynamics. Benthic–pelagic coupling encompasses cycling of particles and solutes between the water column and the sediments through particulate water-column production, settling, sinking, deposition, resuspension, burial, mineralization, regeneration, and pore water exchange (Fig. 1). Any factor that is involved in these processes can affect nutrient and contaminant cycling, ecosystem dynamics, community composition and faunal abundance, and overall water

*Email: porter@cbl.umces.edu

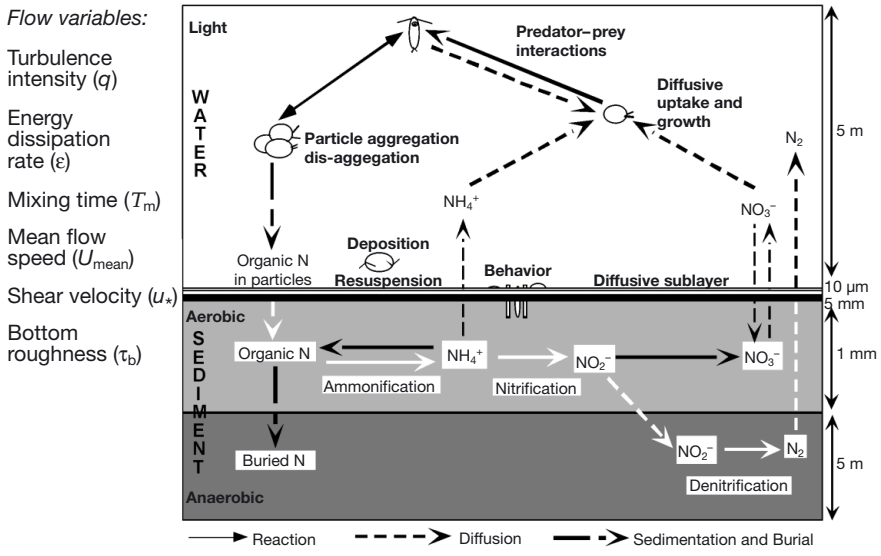

Fig. 1. Nitrogen cycle (N-cycle modified after Henriksen & Kemp 1988) example of benthic–pelagic coupling processes as directly and indirectly affected by water flow. Many of the illustrated processes occur at different spatial and temporal scales

quality in the ecosystem (Tenore et al. 1982, Jensen et al. 1990, Santschi et al. 1990, Caffrey et al. 1993, Cerco & Seitzinger 1997). One of these factors, often ignored in benthic–pelagic coupling studies, is the amount of light that reaches the sediment surface. Another is the hydrodynamics of the sediment–water interface and the overlying water column, which are integral to many aspects of benthic–pelagic coupling (Fig. 1).

Sanford (1997) identified flow variables that should be considered together for realistic experimental ecosystem studies that require hydrodynamic benthic–pelagic coupling. These variables include turbulence intensity (q) and energy dissipation (ε) that are important for water-column processes, and bottom shear velocity (u_*) and mean flow speed (U_{mean}) that are important at the sediment–water interface. Since water-flow variables in the water column and at the bottom boundary-layer are not independent of each other, the ratios of water column and boundary-layer flow must also be scaled appropriately. For example, in natural boundary-layer flows, water-column turbulence intensity and bottom shear velocity scale in a ratio of about 1.4:1. In addition, natural mean flow speed at 1 to 2 m above the bottom and the bottom shear velocity scale in a ratio of about 19:1 (Table 1).

Causal relationships uncovered by studying processes either in the water column (e.g. Sullivan et al. 1991) or at the sediment–water interface (Boynton et al. 1981, Maa et al. 1993, Gust & Müller 1997) have yielded valuable insights. However, such studies may ignore possible direct and indirect linkages and feedbacks in the ecosystem as a whole. Studies have often focused on isolated processes with preferred transport directions or pathways, using either benthic flux chamber type devices or flumes for sediment–water interface process studies (e.g. Boynton et al. 1981, Maa et al. 1993, Thomsen & Flach 1997). Likewise, other studies have focused exclusively on pelagic processes using mesocosms, basins, and bags, with and without considering water flow and mixing (Sanford 1997) and with or without benthos (Sullivan et al. 1991). Scaling of results from studies focused on isolated processes to full natural systems has been questioned (Schindler 1998, Haag & Matschonat 2001) and the flow environ-

Table 1. Scaling relationships for water-column and benthic flow parameters derived from previous studies reporting mean flow speed (U_{mean}), turbulence intensity (q), and shear velocity (u_*) in natural shallow-water environments. Water-column turbulence intensity and benthic shear velocity scale in a ratio of about 1.4:1 in natural shallow-water environments

Instrument	Location	Depth (m)	U_{mean} (SD) (cm s^{-1})	q (SD) (cm s^{-1})	u_* (cm s^{-1})	Scaling relationships $q:u_*$	$U_{mean}:q$	$U_{mean}:u_*$	Source
Model		5.1[a], 20[b]	60[a], 68.4[b]	4.3[a,b]	3[a,b]	1.49[a,b]	14[a], 15.9[b]	20[a], 22.8[b]	Baumert & Radach (1992)
Ducted current meters	Skagit Bay, WA	16	45.87	4.1	2.82	1.5	11.2	16.3	Gross & Nowell (1983)
Electromagnetic current meter	Long Island Sound	52	40 (40)	5 (5)		–	8	–	Bohlen (1977)
Pivoted vane	Choptank River, MD (estuary)	7.5	52.6 (6.6)	3.42	2.51	1.41	15.4	21.0	Gordon & Dohne (1973)
Electromagnetic current meter	off Anglesey, North Wales	12–22	50	4.85	3.6	1.34	10.3	13.9	Bowden (1962)
	Average scaling relationships in natural shallow environments:					1.4	11.1	18.8	

ments of the water column, the benthos, or both have often been mismatched. Results from field approaches are most realistic, however, they are often too variable and uncontrolled (de Wilde 1990) to be conclusive (e.g. Dame & Libes 1993) or may require multi-decadal or global sampling (e.g. Sebens 1994) to discern statistically acceptable cause–effect relationships.

Because of design artifacts and inappropriate extrapolation across scales, mesocosm approaches have often been criticized (Bruckner et al. 1995, Carpenter 1996, Duarte et al. 1997, Asmus et al. 1998, Kampichler et al. 2001). In fact, data generated in standard isolated tank mesocosms can lead to discrepancies in predictive ecosystem models (Vallino 2000, Watts & Bigg 2001). Realistic water flow and turbulent mixing have not been considered sufficiently in mesocosm design (Sanford 1997), nor has the scaling between water-column turbulence and benthic boundary-layer flow (Porter 1999, and present Table 1). Bottom shear, a variable that controls many processes at the sediment–water interface, is unrealistically low in standard mesocosms (Crawford & Sanford 2001) and may cause artifacts in the results of benthic–pelagic coupling studies.

It is technically challenging to produce both realistic water-column turbulence and realistic benthic boundary-layer flow in a single system, because the benthic and pelagic flow and turbulence parameters do not scale linearly. For example, typical mesocosm mixing mechanisms often result in unrealistically low bottom shear when water-column turbulence is set to realistic levels. Any increase in water-column mixing in order to increase bottom shear stress very quickly increases water-column turbulence to unrealistic levels. In addition, the mixing schemes used in many experiments are often not fully documented. Water columns and sediment compartments have been linked in the past (e.g. Perez et al. 1977, Prins et al. 1995, 1997); however, this was done without any considerations of scale, hydrodynamics, and possible alteration of feedbacks selected in the experimental setup. Nevertheless, Threkheld (1994) urged a balanced view of pelagic and benthic processes, and Perez et al. (1977) emphasized the importance of appropriate physical and biological scaling in ecosystem experiments to correctly represent both water-column and benthic processes including any indirect links.

Our primary objectives in this study were to determine (1) if an improved experimental ecosystem could be designed that mimics shallow-water processes more closely with both realistic water-column turbulence and benthic boundary-layer flow in a single linked system, (2) how an improved representation of benthic boundary-layer flow can affect benthic–pelagic coupling processes in ecosystem experiments, (3) if the unrealistically low bottom shear in standard mesocosms is an artifact of mesocosm studies that cannot be ignored, and (4) how mesocosm shape can affect ecosystem results.

In this study, we designed and built linked mesocosms that were scaled to typical isolated tank mesocosms but included improved bottom-flow characteristics. We then quantified the water-column and bottom-flow characteristics in 2 sets of systems with 2 different shapes, and assessed variables such as light, water-column nutrient levels, sediment nutrient flux rates, phytoplankton biomass, and oyster growth rate from comparative ecosystem experiments. This study was part of a more complex ecosystem study examining the interaction of bivalve suspension-feeders and water flow on benthic–pelagic coupling processes and its impact on overall water quality, with particular focus on the effect of oysters and enhanced bottom shear velocity on water quality in Chesapeake Bay, Maryland, USA (Porter et al. 2004, this issue).

MATERIALS AND METHODS

We designed and built 2 scaled, linked mesocosm systems, and scaled water-column turbulence levels to be the same in the linked mesocosms and their respective isolated tank counterparts. In addition, we established a realistic bottom shear velocity (bottom shear stress) in the linked mesocosms to compare with the unrealistically low bottom shear velocity in the standard isolated tanks. Finally, we tested the effect of enhanced bottom shear velocity on benthic–pelagic coupling processes in comparative, scaled, replicate ecosystem experiments.

Systems design. A schematic of the linked and isolated mesocosm systems with 100 l and 1000 l water volume and a sediment surface area of 0.1 and 1 m^2, respectively, all made of fiberglass, PVC, and acrylic, is shown in Fig. 2. The large and small isolated tanks (Fig. 2a,c) consisted of 1 m deep cylindrical tanks with diameters of 1.13 and 0.35 m, respectively. The large and small tanks were uniformly mixed by sets of impellers on shafts that extended vertically into the center of the tanks. The impeller blades of the large tank were located 25 and 75 cm from the water surface, were 8 cm wide, and were tilted at a +45° angle to the surface. The impeller blades of the small tank were located 18, 34, 51, 67 and 83 cm from the water surface, were 8 cm wide, and were also tilted at a +45° angle to the surface. The impellers were driven by overhead direct-current motors and swept the inner half diameter of the tanks at 3.75 rpm in the large tank and 10 rpm in the small tank. To prevent plug flow, the impellers were programmed to rotate in one direction for 7 revolutions, stop for 15 s, rotate in the opposite

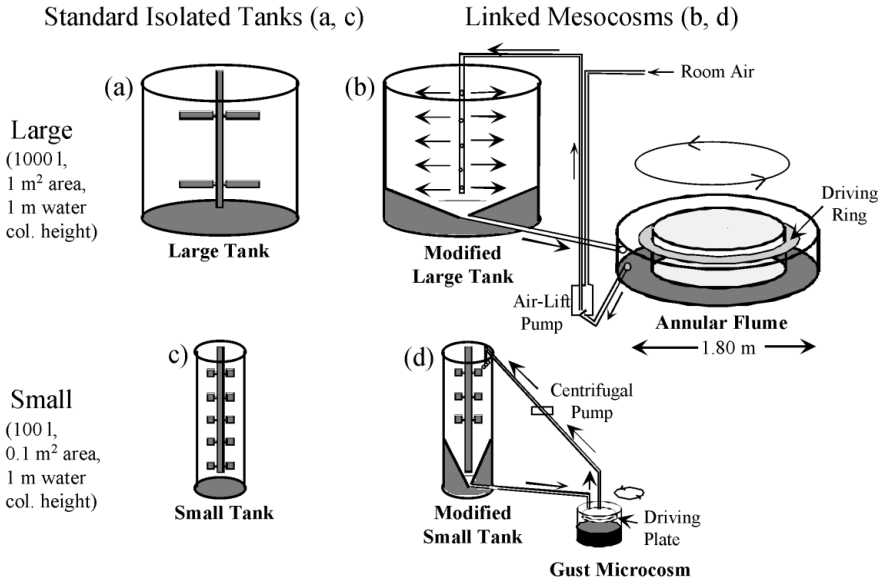

Fig. 2. Experimental ecosystem configurations. In the linked mesocosms, benthic boundary-layer devices were linked to modified water-column tanks to mimic flow both in the water column and at the sediment–water interface more realistically than in the isolated tanks. These setups were also used in our sequential ecosystem experiments with oysters in all 4 systems a–d, there defined as: (a) large isolated tank with bivalves = L+b; (b) large linked mesocosm with bivalves and benthic boundary-layer flow = L+b+f; (c) small isolated tank with bivalves = S+b; (d) small linked mesocosm with bivalves and benthic boundary-layer flow = S+b+f. Tanks without oysters also run during the ecosystem experiments are defined as large isolated tank = L, small isolated tank = S

direction for 7 revolutions, stop for 15 s, and repeat the cycle continually for 4 wk long ecosystem experiments with tidal cycling in a 4 h on and a 2 h mixing-off mode.

The linked mesocosms had the same water volume, sediment surface area, and water column height as the isolated tanks. The large and small linked mesocosms consisted of modified water-column tanks each exchanging fluid with a benthic boundary-layer device at rates of 13.6 l min^{-1} in the large linked mesocosm and 11.6 l min^{-1} in the small linked mesocosm devices (Fig. 2b,d). The large system consisted of a tank with a funnel-shaped bottom linked to an annular flume (Fig. 2b) that had an outer diameter of 1.80 m, a 20 cm wide channel, and a 15 cm water-column height. Water flow in the flume was driven by a transparent, rotating, inner half ring skimming the water surface, suspended from aluminum spokes connecting to a motor similar to that of Maa et al. (1993). For fine control of the lid speed, a gear box with a ratio of 100:1 was used, and was coupled to an electronic computer control. Several techniques are available to reduce secondary circulation in annular flumes, including the use of a lid cover reduced in size (Deardorff & Yoon 1984), as used here. In addition, the aspect ratio (outer flume diameter divided by channel width) was kept at a value of 9 to further reduce secondary circulation (Sheng 1989). Both design features resulted in low secondary flow, less than 7.2% of the mean velocity as determined by an Acoustic Doppler velocimeter at different ring speeds (Porter 1999), and a relatively homogeneous bottom shear stress generated by the lid rotation. The small linked system consisted of a small tank with a funnel-shaped bottom connected to a 40 cm diameter Gust microcosm (Gust & Müller 1997) as the bottom shear-generating benthic boundary-layer device (Fig. 2d).

Water passed between the benthic and pelagic compartments of these systems through a pipe with a valve, a level sensor, and a pump. Water-column mixing in the large linked tank was induced by pulsed jet flow using a 2.5 l air-lift pump (designed after K. T. Perez & E. W. Davey pers. comm.). In the small linked tank, water-column mixing was induced by an overhead motor driving impeller blades located 18, 34, and 51 cm from the water surface. Further details of the design of the systems and the designs of the connections can be found in Porter (1999). Mixing cycles of all systems were electronically synchronized in all our experiments.

Scaling of internal mixing and benthic boundary-layer flow. We chose water-column turbulence intensity levels (q) of 1 cm s^{-1} as our target in all systems, with q defined in Tennekes & Lumley (1972) as

$$q = \sqrt{\tfrac{1}{3}(\langle u^2\rangle + \langle v^2\rangle + \langle w^2\rangle)} \quad (1)$$

Here $\langle u^2\rangle$, $\langle v^2\rangle$, and $\langle w^2\rangle$ are the variances of their respective velocity components. This value of q is at the lower end of intensities in natural systems, and allowed energy dissipation rates in the systems to remain at reasonable levels.

The target bottom shear velocity was moderate at 0.6 cm s^{-1}. Low bottom shear velocities were found (~0.1 cm s^{-1}) in the isolated tanks at water-column turbulence intensities of 1 cm s^{-1} (Crawford & Sanford 2001). With a turbulence intensity of 1 cm s^{-1}, a target bottom shear velocity of 0.6 cm s^{-1} is required to simulate the pelagic–benthic relationship of q:u_* (1.4:1). This pelagic–benthic relationship of q:u_* of 1.4:1 is consistently found in shallow environments in nature (see Table 1). A moderate shear velocity of 0.6 cm s^{-1} was chosen to avoid large-scale sediment erosion while

avoiding diffusion limitation at the sediment–water interface.

We used a combination of gypsum dissolution techniques and direct flow/turbulence measurements with an acoustic Doppler velocimeter (ADV) to determine turbulence intensities at different mixing speeds at a number of representative locations in our experimental ecosystems. While they are not a universal integrator of 'water motion', under certain flow and turbulence conditions gypsum dissolution techniques can be used to obtain volume-weighted estimates of turbulence intensity or mean flow speed (Porter et al. 2000). The isolated tanks and the small linked water column tank qualified as fluctuating-flow environments, the benthic boundary-layer devices were steady flow environments, and the large linked mesocosm was a mixed-flow environment as defined in Porter et al. (2000). We determined volume-weighted turbulence intensity as a function of mixing speed from dissolution rates of 3 cm diameter gypsum spheres for representative locations in the isolated tanks and in the benthic boundary-layer devices (Porter et al. 2000, Crawford & Sanford 2001). The gypsum sphere locations were selected based on their distance from the mixing devices. The spheres were calibrated in the fluctuating-flow (FF) and steady-flow (SF) environments, respectively (FF: q = 16.49 × dissolution rate – 1.08 [R^2 = 0.81]; SF: q = 0.80 × dissolution rate – 0.40 [R^2 = 0.98]); calibration equations from Porter et al. (2000).

In the large linked tank, in which dissolution techniques are inappropriate (Porter et al. 2000), turbulence intensity was measured with an acoustic Doppler velocimeter at 50 regularly spaced locations at 3 mixing speeds. Using a Kriging technique in Surfer (Golden Software) we determined the volume-weighted turbulence intensity at the respective mixing speeds for all systems. From linear regression analysis of all intensities and all mixing speeds, an overall volume-weighted turbulence intensity of 1 cm s^{-1} was obtained for each experimental ecosystem. Local turbulence levels in the mesocosm systems are shown in Fig. 3. Volume-weighted energy dissipation rates (ε) were calculated from velocity measurements using equations from Sanford (1997).

Scaling of benthic flows. We used a combination of qualitative, quantitative, and semi-empirical engineering techniques (see below) to determine the benthic shear velocities in our 4 experimental ecosystems.

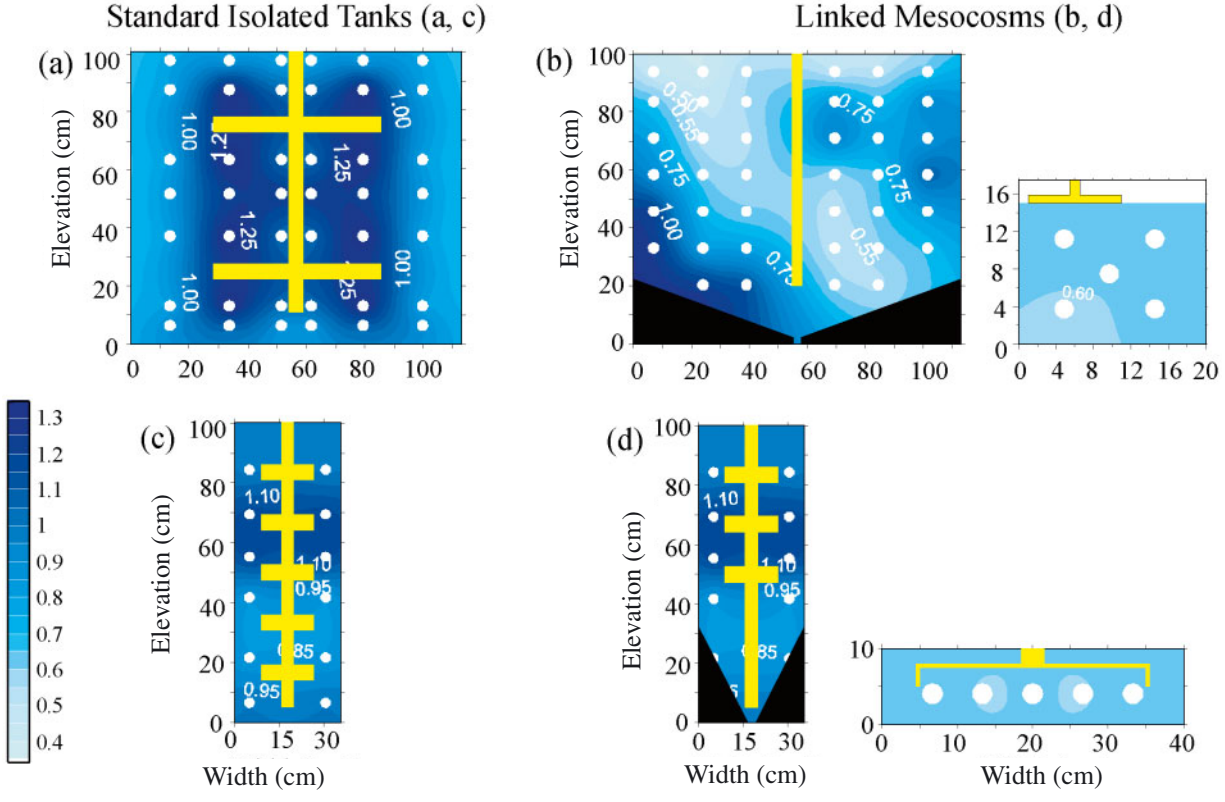

Fig. 3. Turbulence intensities were uniform and similar in large and small isolated tanks (a,c) and in the large and small linked mesocosms (b,d) with a volume-weighted average of about 1 cm s^{-1} in all systems. The scale of the benthic boundary-layer devices is expanded by a factor of about 3 for the Gust microcosm and of about 4 for the annular flume, for clarity

Shear (or 'friction') velocity ($u_\star$) expresses the boundary-layer shear stress on a velocity scale

$$u_\star = \sqrt{\frac{\tau_b}{\rho}} \quad (2)$$

where τ_b is bottom shear stress and ρ is the density of water. Benthic shear velocity is generated by velocities in the water column that may include steady flows, transients, waves (Terray et al. 1996), or stirring such as in our isolated tanks. In most natural environments the shear velocity is created by wall-bounded shear flow. The mechanism used to create benthic shear in our linked systems was that of lid-driven steady flow.

Benthic shear velocity measurements. Shear velocity was quantified directly at the bottom of the isolated tanks, the Gust microcosm, and the annular flume using hot-film anemometry (Ludwieg & Tillman 1949, Fingerson & Freymuth 1983, Gust 1988). Shear velocities and their homogeneity across the bottom of the Gust microcosm were calibrated over 9 settings from 0.29 ± 0.01 to 1.24 ± 0.03 cm s^{-1} in an automated hot-film test facility at the Technische Universität Hamburg-Harburg, Germany (Gust & Müller 1997). For use in other mesocosm tanks and the annular flume we constructed shear-stress sensors following Gust (1988), using Type WT G-50A sensors from Micro Measurements and constant-temperature anemometry cards (TSI PN 2605462 Rev. B) with a selected overheat ratio of 1.05 (at 20.5 and 20.8°C). Data were recorded as voltage output on a Tattletale Model No. 2 datalogger at a sampling rate of 20 Hz. The mean voltage output of the shear stress sensors was calibrated to known shear velocities at the operational temperature settings in the Gust microcosm of 20.5° and 20.8°C, i.e. the temperatures at which measurements were taken in the systems. Shear velocities in the small and large tanks were measured at 2 mixing speeds and different radial positions at the bottom of the tanks (Crawford & Sanford 2001). In the flume we excluded some shear stress sensor measurements due to sensor, cabling, and anemometer card problems, however, 17 successful shear velocity measurements at different locations across the flume channel were obtained and averaged for each rpm increment. For the annular flume, not enough hot-film data were available to obtain a complete spatial distribution of bottom shear across the sediment surface. An averaged shear velocity of 0.48 ± 0.23 cm s^{-1} was obtained from 17 data locations, which is consistent with results from additional measurement methods which provided a $u_\star$ of 0.6 cm s^{-1} (initiation of sand motion with known d50) and 0.7 cm s^{-1} (drag coefficient calculation), respectively (Porter 1999). Commonly applied techniques to determine shear velocity in linear flumes such as the log-layer technique (Nowell & Jumars 1984, Muschenheim et al. 1986, Mann & Lazier 1991) cannot be used in annular flumes since the driving mechanism leads to non-logarithmic vertical velocity profiles with secondary circulation.

Comparative ecosystem experiments in the systems that only differed in shear velocity. To test the working hypothesis that ecosystem processes may differ in linked compared to isolated tank mesocosms, we performed 3 ca. 4 wk long ecosystem experiments using the systems in Fig. 2 with muddy sediment and oysters and an additional isolated tank in each series without oysters. The experiments were performed 3 times in sequence with Expt 1 performed in summer 1995, Expt 2 in fall 1995, and Expt 3 in spring 1996. In this series of experiments, the position of each of the 3 treatments (i.e. a, b, c in Fig. 4) was rotated to follow the pattern of a latin square (Steel & Torrie 1980, present Fig. 4). Our 3 treatments consisted of an isolated tank with oysters, a linked mesocosm with oysters, and an isolated tank without oysters. This experimental design was duplicated in the large and small systems. In a pilot experiment in the large systems without oysters (Porter 1999), phytoplankton biomass was similar between the isolated tanks and the linked mesocosm.

Sediment was collected from a local estuary into a holding tank and covered with black plastic for 4 d to render it anaerobic. It was then distributed into trays that fit the mesocosms, scraped flat, and kept in flow-through filtered estuarine water in the dark for 14 d. In a separate study we found that this procedure produces defaunated sediments and produced realistic porewater gradients in the sediment (Porter 1999).

At the start of each experiment, the sediment trays were placed into all 1000 and 100 l mesocosms, giving a 10 cm sediment layer. The systems were then filled with unfiltered estuarine water from the Choptank River, a tributary of the Chesapeake Bay, and appropriate scaled biomasses of oysters *Crassostrea virginica*, 28.8 g total live weight of juvenile (about 2.5 cm long) oysters per 100 l water volume, were added and distributed randomly across the sediment bottom. There were about 13 individual oysters in the small systems and about 130 in the large systems.

	Position		
Expt 1	a	b	c
Expt 2	b	c	a
Expt 3	c	a	b

Fig. 4. Experimental design of a latin square analysis of variance (adapted after Steel & Torrie 1980). For each experiment, position of each tank (i.e. a, b, c) was changed to a different location to eliminate location effects

The experiments were housed indoors. Illumination was provided from light banks above the tanks with broad spectrum fluorescent bulbs on a simulated day–night cycle of 12:12 h light:dark. Daylight levels at the water surface were set to about 160 µE m^{-2} s^{-1}. Water temperatures in the experiments were 22 ± 1°C. Illumination of the sediment surface of the linked systems was adjusted using shading mesh by extrapolating vertical light profiles in the water column tanks to 1 m depth. To mimic tidal exchange, we replaced 10% of the water in each system daily with 0.5 µm-filtered estuarine Choptank river water. Within the first 3 d of each experiment we added a nutrient spike of ammonium and soluble reactive phosphorus (SRP) at the Redfield ratio to all systems, which increased initial ammonium and SRP levels in the tanks by about 25 and 1.6 µM, respectively. Throughout the experiments, all system side walls were cleaned of wall periphyton biweekly (more often when needed) to prevent any bias in the results (Chen et al. 1997, 2000).

Biological and geochemical variables were measured throughout the experiments. These were water-column chlorophyll *a*, water column nutrient concentrations of SRP; ammonium, nitrate + nitrite, dissolved inorganic nitrogen (DIN), silicate, oyster growth rate, and light levels at the sediment surfaces together with sediment chlorophyll *a*. Pre- and post-experiment dissolved inorganic nitrogen fluxes from the sediments were determined from sediment incubations.

We measured water-column chlorophyll *a* as an indicator of phytoplankton biomass every 2 to 3 d, and used fluorometric analyses following extraction with acetone (Lorenzen 1967) and sonication from Whatman GFF glass-fiber filters. Water-column nutrient concentrations were measured every 2 to 3 d, and the data from all experiments from 2 d after the spike until the end of the experiment were included in statistical analyses. Water-column SRP concentrations were measured every 2 to 3 d and averaged per time span from shortly after the nutrient addition until depletion occurred. To determine oyster growth rate over each experiment, individual oysters were marked and their live weight measured before and after each experiment. Light profiles were measured every 2 to 3 d at 0, 25, 50, 75 cm using a Li-Cor light meter, and light at the sediment surface was determined following Parsons et al. (1984):

$$I_d = I_0 \times e^{-kd} \quad (3)$$

Chlorophyll *a* concentration in the surface sediment as an indicator of microphytobenthos biomass was measured at the end of Expts 2 and 3 but not at the end of Expt 1. After observing mass erosion events and bubble formations in previous experiments, we implemented weekly sediment chlorophyll *a* measurements in Expt 3. The 0 to 0.5 cm surface sediment layer was sampled using 2.5 cm diameter coring devices and kept frozen at −80°C until analysis. Extraction was done using acetone and sonification, with subsequent analysis by high-performance liquid chromatography (Van Heukelem et al. 1992, 1994).

At the end of the mesocosm experiments, we removed sediment cores from the mesocosms using 3 replicate 13.3 cm diameter, clear, acrylic benthic chambers per system. We then added filtered water to the benthic chambers, sealed the chambers air-tight, added stirring, and incubated the cores first in the dark and then in the light to obtain sediment DIN dark and light sediment flux rates and a net dark + light flux rate for each chamber. DIN flux rates from the sediments were corrected for water-column processes using data from chambers run without sediment. We did not determine sediment DIN flux rates in the light for Expt 1 but did so for Expts 2 and 3. Sediments at the start of an experiment were taken from the flow-through water bath and incubated in the dark only.

Latin square analyses of variance included the data of a variable from all experiments in the analysis, and were performed on these variables: water-column chlorophyll *a*, water-column nutrient concentrations (SRP, nitrate + nitrite, DIN, silicate). Responses for sediment flux cores with dark and light incubations added a split-plot or repeated-measures dimension to the design (sediment DIN fluxes). Responses that were quantified by rates that are described by regression lines were analyzed by multivariate analysis of variance (MANOVA) with the slope and intercept as the dependent variables (water-column nutrient concentrations). Analysis of variance was applied to individual experiments when data for 1 of the 3 experiments were lost (sediment chlorophyll data from Expt 1) or not measured (sediment DIN flux rates in the light in Expt 1), and repeated significant effects of the same direction over multiple experiments were taken as indicative of an overall effect. Statistical analyses were performed using SAS (SAS Institute). In Expt 1, the Gust microcosm decoupled from the tank on Day 12 and data from the small linked mesocosm after Day 12 were excluded.

RESULTS

Scaling of water-column mixing and benthic boundary-layer flow

Volume-weighted turbulence intensity (q) was the same in all systems at about 1 cm s^{-1} (Table 2). Turbulence intensities were uniform in all systems but were slightly higher near the turbulence-generating pad-

Table 2. Volume-weighted results for measured benthic boundary-layer flow and water-column turbulence variables in our large and small linked mesocosms and in their isolated tank counterparts. Water-column and benthic flow ratios were measured in our mesocosms at the operational mixing-on settings. Ratio of turbulence intensity to shear velocity in our linked mesocosms was similar to the value of 1.4:1 in natural shallow-water environments (cf. Table 1). However, it was distorted at ≥7:1 in the isolated tank systems that had the same realistic turbulence intensities of about 1 cm s^{-1} but much reduced benthic shear velocities. ADV: acoustic Doppler velocimeter; q: turbulence intensity; ε: energy dissipation rate; U_{mean}: mean flow speed; and u_*: benthic shear velocity

System	Instrument	Depth (m)	U_{mean} (cm s^{-1})	ε (cm^2 s^{-3})	q (cm s^{-1})	u_* (cm s^{-1})	Scaling relationships q:u_*	U_{mean}:q	U_{mean}:u_*
Large linked mesocosm	ADV, shear stress sensors	1	9.92	0.02	0.75	0.481 (± 0.234)	1.6	13.2	20.6
Small linked mesocosm	ADV, shear stress sensors	1	10.4	0.03	0.94	0.588 (± 0.01)	1.6	11.0	17.7
Large isolated tank	ADV, shear stress sensors	1		0.02	0.95	0.127 (± 0.021)	7.5	–	–
Small isolated tank	ADV, shear stress sensors	1		0.03	0.99	0.141 (± 0.017)	7	–	–

dles in the large isolated tanks, decreasing towards the walls and the bottom. They were highest near the bottom in the linked systems (Fig. 3). Volume-weighted energy dissipation rates were realistic, with about 0.02 cm^2 s^{-3} in the large and 0.03 cm^2 s^{-3} in the small systems, respectively (Table 2). Mean shear velocities in our linked large and small systems reached the moderate target shear velocity of about 0.6 cm s^{-1} (Table 2), whereas in the isolated large and small tanks shear velocities were generated at only about 0.13 cm s^{-1}.

Whereas the shear velocities in the benthic boundary-layer devices of the linked mesocosms were generated by sheared mean flow, the bottom stresses in the isolated tanks were generated by velocity fluctuations in the overlying water column induced by stirring. Mean flow speeds amounted to ~10 cm s^{-1} in the linked mesocosms (Table 2) whereas they were lower than 2 cm s^{-1} in the isolated tanks. The scaling relationship of water-column turbulence intensity to benthic shear velocity of about 1.4:1 found in natural shallow-water environments (Table 1) was approximated closely at about 1.6:1 (Table 2) in our large and small linked mesocosms, but was far off at 7.5:1 in the large and small isolated tanks (Table 2). Thus, as planned, the large and small linked systems met the design requirements, and the only hydrodynamic differences between the isolated tanks and the linked systems were type and intensity of the benthic boundary-layer flow and bottom shear velocity. This experimental set-up now permitted a true comparative study of ecological responses to both different types of hydrodynamic coupling and stronger (more realistic) benthic shear velocity/stress.

Differential effects on ecosystem function

Here we present ecosystem results, with oysters present in all systems as the default unless specified otherwise.

The shape of the small systems limited penetration of light through the water column and to the sediment surface due to shading by the walls, whereas the shape of the large systems did not (Fig. 5), and the significant effects of light availability on ecosystem processes dominated all comparisons between the large and the small systems. Light in the water column significantly increased phytoplankton abundance (Fig. 6; as chlorophyll *a* content) and thus food availability for the oysters in the large systems. However, phytoplankton levels were also low over long periods of time in the large system. Overall, oysters grew significantly better in the large systems than in the small systems (Fig. 7). Whereas water-column nutrients from the added nutrient spike at the start of the experiment were taken up in the large systems and nutrient levels decreased over the duration of each experiment, nutrient levels (e.g.

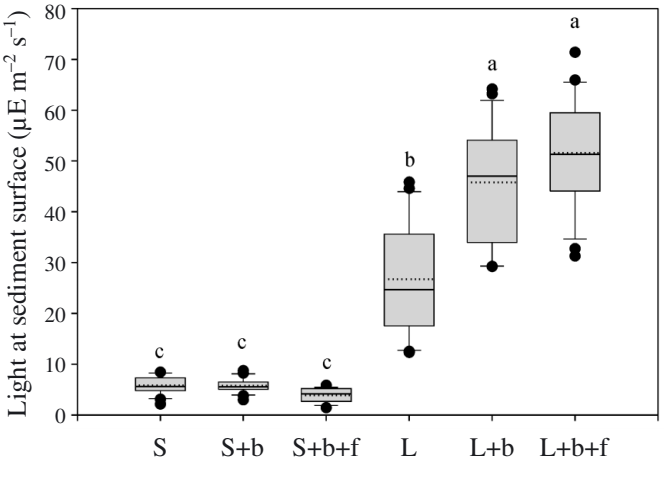

Fig. 5. Box-whisker plot of light levels at sediments of large and small systems during all experiments and integrated over time for large and small systems. Results from latin square ANOVA of the 3 experiments, with significant differences ($p < 0.05$) depicted by letters. Treatment abbreviations as in Fig. 2 legend. Median (line), mean (dotted line), 25 and 75% quantiles (bars), and 10 and 90% quantiles (whiskers) are shown; (●) outliers

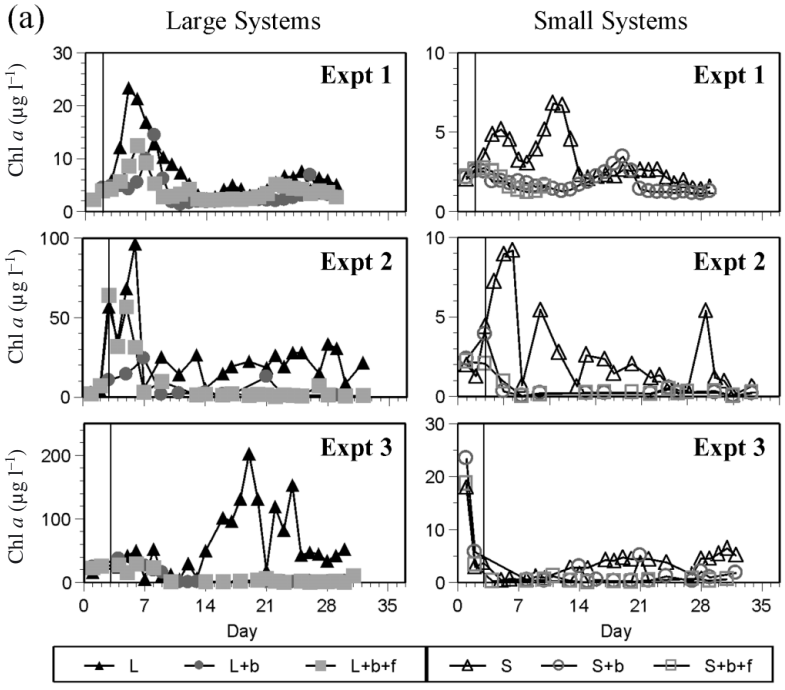

(b)

Comparison	Water Column Chl *a*
a. L+b *vs* L+b+f	p = 0.2580
S+b *vs* S+b+f	p = 0.1256
b. L *vs* S	**p = 0.0021**
L+b *vs* S+b	**p = 0.0019**
L+b+f *vs* S+b+f	**p = 0.0003**

Fig. 6. (a) Water-column chlorophyll *a* levels over time in large and small systems during 3 sequential mesocosm experiments; note different scales of *y* axes. Vertical line: time when oysters and nutrients were added. (b) Results from latin square ANOVA of the 3 experiments. Treatment abbreviations as in Fig. 2 legend

nitrate + nitrite) remained high or increased throughout the experiments in the small systems (Fig. 8). Overall, water-column nutrient concentrations were significantly higher in the small than in the large systems (Fig. 8).

Whereas sediment chlorophyll *a* abundance (an indicator of microphytobenthos abundance) was light-limited and low in the small systems, it was not light-limited and significantly higher in the large systems (Fig. 9). Increased benthic shear velocity significantly decreased sediment chlorophyll *a* abundance in the large systems. Although sediment chlorophyll *a* abundance differed between experiments, it was repeatedly significantly higher in the large isolated tank than in the large linked mesocosm at the end of each experiment (Fig. 9). We noticed a period of gas formation in the microphytobenthos mat in the annular flume over the first few weeks of the experiments, followed by mass erosion of sediment chlorophyll *a* in Week 4, but we only performed weekly sediment chlorophyll *a* measurements in Expt 3. This phenomenon is shown in the weekly sediment chlorophyll *a* abundances in Expt 3 of the large system (Fig. 10) and represents a microphytobenthos mass erosion event, initiated both by sufficiently high bottom shear velocity and destabilizing gas production (i.e. a decreased critical shear stress with increasing age of the mat). Thus, system shape, benthic shear velocity, and the age of the mat all significantly affected microphytobenthos biomass.

Microphytobenthos on the surface of the 10 cm sediment layer in the large systems significantly affected the direction of sediment DIN fluxes into or out of the sediments at the end of the experiments (Fig. 11), thus significantly affecting the nutrient feedbacks from the sediments to the water column. Because we performed all sediment flux experiments without oysters and used blank water column chambers as controls to subtract water-column activity, we were able to attribute any observed flux rates and their directions to the sediment

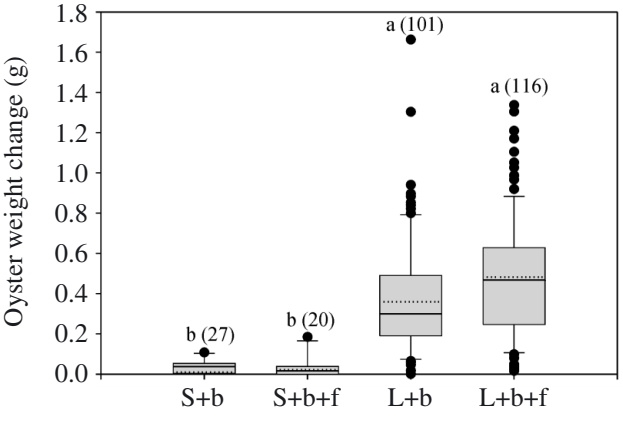

Fig. 7. Live total individual oyster weight changes over all experiments and integrated over time for large and small systems. Numbers in parentheses: numbers of oysters recovered after an experiment that were included in analysis; lowercase letters above bars indicate results from ANOVA and Student-Newman-Keuls analysis of the data at $p < 0.05$, whereby different letters indicate significant differences between the data. Box plot; top whisker = 90th percentile and top bar 75th percentile; solid line = median; dotted line = mean; bottom bar = 25th percentile and bottom whisker 10th percentile; (●) outliers. Treatment abbreviations as in Fig. 2 legend

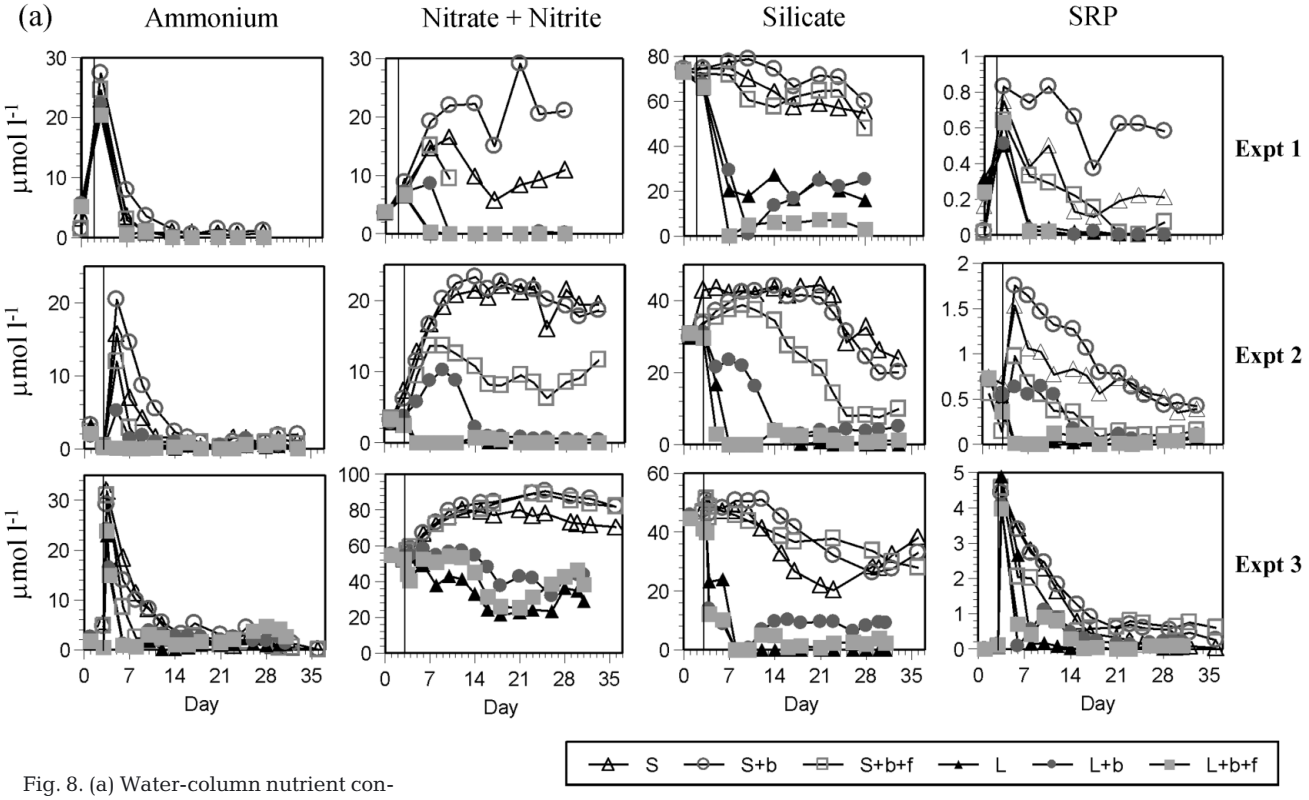

Fig. 8. (a) Water-column nutrient concentrations over time in large and in small systems in 3 sequential experiments. (b) Results from latin square ANOVA of the 3 experiments for the nutrients in (a) and for water-column dissolved inorganic nitrogen (DIN). SRP: soluble reactive phosphorus. Vertical line: time when oysters and nutrients were added. Treatment abbreviations as in Fig. 2 legend

(b)

Comparison	Ammonium	Nitrate+nitrite	DIN	Silicate	SRP
a. L+b *vs* L+b+f	p = 0.6996	p = 0.7133	p = 0.6978	p = 0.2547	p = 0.4128
S+b *vs* S+b+f	**p = 0.0001**	p = 0.3214	p = 0.2276	p = 0.2505	**p = 0.0042**
b. L *vs* S	**p = 0.0014**	**p = 0.0188**	**p = 0.0142**	**p = 0.0007**	**p = 0.0016**
L+b *vs* S+b	**p = 0.0001**	**p = 0.0192**	**p = 0.0124**	**p = 0.0008**	**p = 0.0004**
L+b+f *vs* S+b+f	p = 0.7466	**p = 0.0550**	**p = 0.0501**	**p = 0.0008**	**p = 0.0256**

and its sediment-associated surface biofilms. Microphytobenthos also significantly affected sediment DIN flux rates between the large isolated tank and the large linked mesocosm in the light, and significantly affected the overall sediment DIN flux rates (dark rate + light rate) between the isolated tank and the linked mesocosm (Fig. 11). Sediment DIN flux rates from sediments before the mesocosm experiments were small (Fig. 11), and thus the sediments were not very geochemically active. Sediment DIN effluxes or small uptakes were observed in the dark in the large systems at the end of the experiments (Fig. 11). DIN uptake in the light by the sediment and its associated micro-

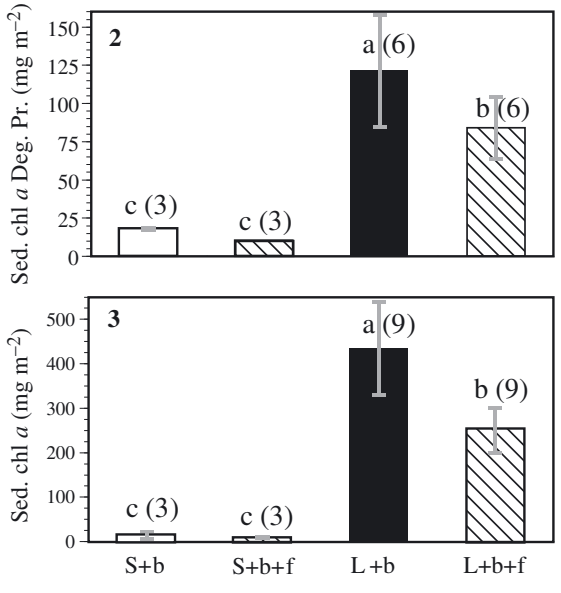

Fig. 9. Sediment chlorophyll *a* concentrations at end of Expts 2 and 3 (data lost for Expt 1). Bars represent mean ± SD sediment chlorophyll *a* abundance; sample size: n = 9 in large systems, 3 in small systems. Lower-case letters above bars indicate statistical results; different letters indicate significant differences. Treatments abbreviated as in Fig. 2 legend

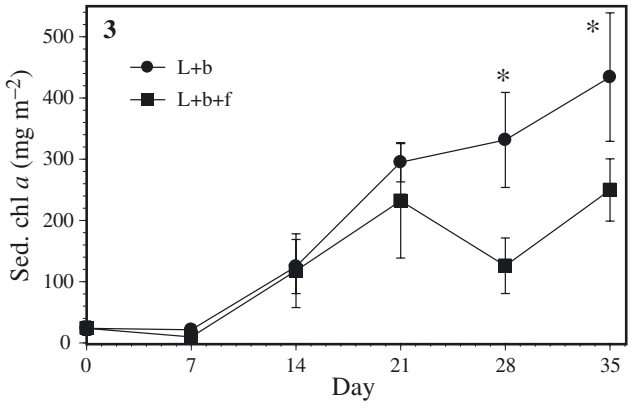

Fig. 10. Mean (± SD) weekly sediment chlorophyll *a* abundance (top 0.5 cm) during Expt 3 in large isolated tank with oysters (L+b) and our large linked mesocosm with oysters (L+b+f) (not measured for Expts 1 and 2). For Day 28 (around which time a mass erosion event was observed) and for Day 35, sediment chlorophyll *a* levels were significantly (∗) reduced in L+b+f treatment. Number of samples: n = 3 in each treatment on Days 0, 7, 14, 21, 28, and n = 9 for each treatment on Day 35

phytobenthic community was repeatedly significantly highest in the large isolated tank (Fig. 11), which also repeatedly had the significantly highest sediment chlorophyll *a* abundance (Fig. 9), whereas DIN uptake by the sediment was repeatedly significantly lower in the large linked mesocosm in which microphytobenthos abundance (as chlorophyll concentration) was significantly decreased due to erosion by increased bottom shear (Fig. 9). The net result for combined sediment dark + light sediment DIN fluxes was a repeatedly significantly higher uptake in the large isolated tanks than in the large linked systems.

In strong contrast to significant sediment geochemical and biological activity at the sediment–water interface in the large systems, in the small systems dissolved inorganic nitrogen sediment flux rates from the sediment to the water column were zero after Expts 2 and 3 (Fig. 11), or only about one-half of the flux rates of the large systems after Expt 1 (Fig. 11). Altogether, sediment biogeochemical and biological activity was low in the small systems.

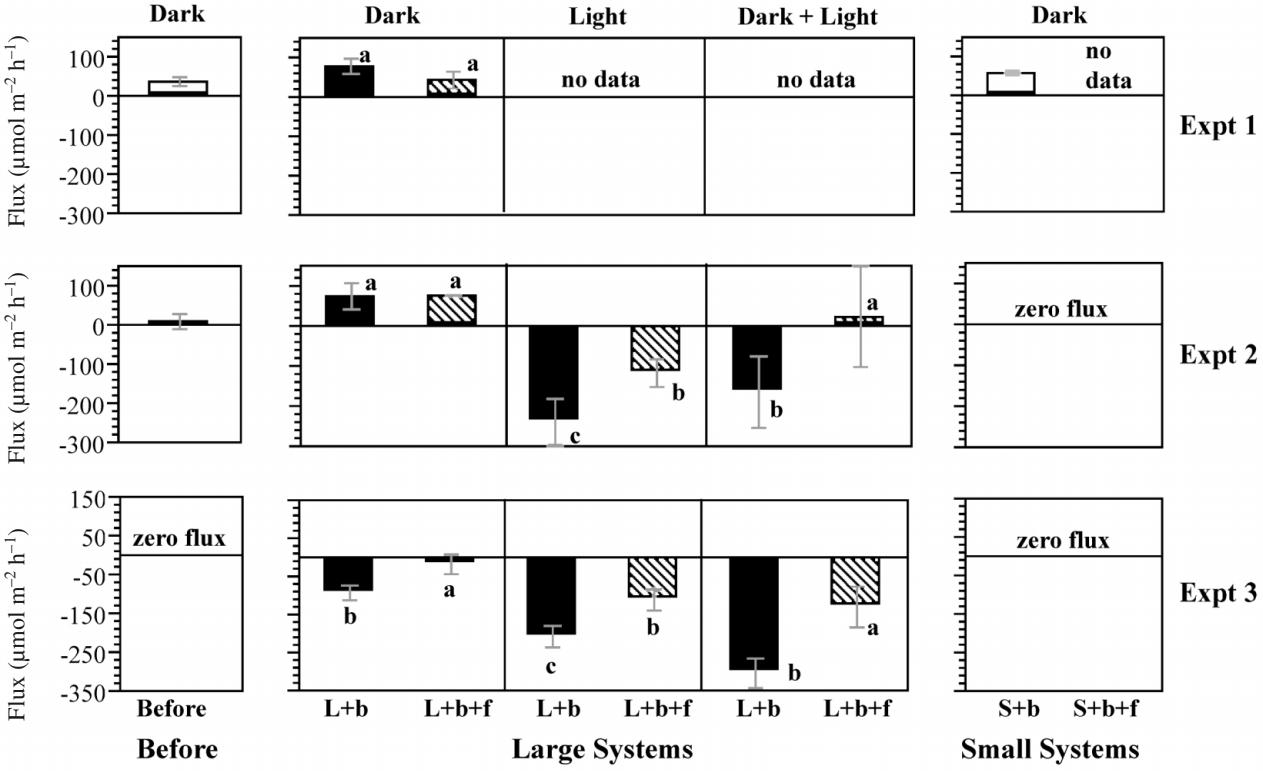

Fig. 11. Mean (± SD) sediment DIN (DIN = NO_2^- + NO_3^- + NH_4^+) flux rates (positive = DIN flux from sediment to water column; negative values = DIN taken up by sediments) before and after the 3 sequential mesocosm experiments with sediment collected from the mesocosms. Sediment incubations were performed in the dark and in the light and were performed without oysters. Dark and light rates are sum of DIN flux rates in dark and in light for net daily estimates of sediment DIN flux for each system. Light incubations were not performed in Expt 1. Different letters indicate significant differences as determined by Student-Newman-Keuls tests at $p < 0.05$ in comparison of dark and light fluxes and in comparison of combined fluxes. Before = cores before mesocosm experiments; n = 3 for all treatments, except n = 2 for L+b+f in Expts 2 and 3, where n = 2. Treatments abbreviated as in Fig. 2 legend. All sediment incubations were carried out without oysters

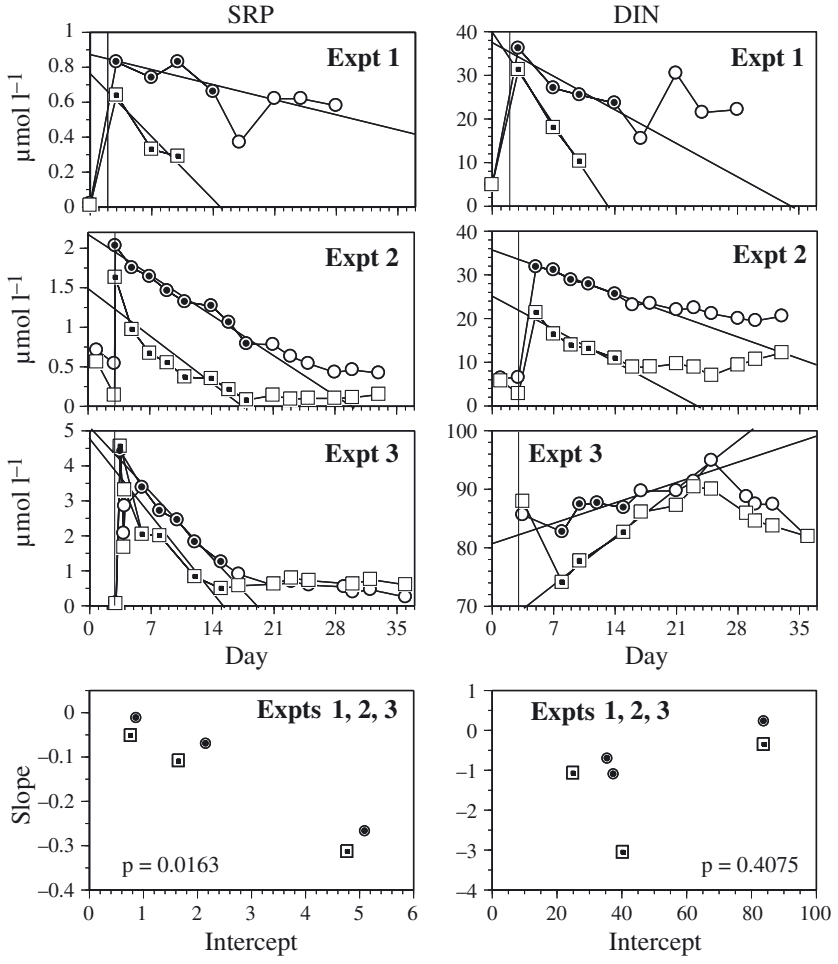

Fig. 12. Top 3 rows: soluble reactive phosphorus (SRP) and DIN concentrations over time in small isolated tank with oysters (○) and small linked mesocosm with oysters (□) in 3 mesocosm experiments. Data indicated by symbols containing dots were used in statistical analyses and to obtain averages, and include time period from shortly after the nutrient spike until nutrient depletion for SRP (Days 3 to 15). Vertical line: time when oysters and nutrients were added. Bottom row: Slopes. For SRP over the 3 experiments, slope was significantly more negative for S+b+f at any given level of intercept, indicating a faster disappearance of SRP from the water-column in S+b+f than in S+b. There was no significant slope-intercept correlation for water column DIN. Conservative statistical measure, Pillai's trace, was used to determine statistical significances in the MANOVA

We found significant differences in water-column nutrient dynamics between the small isolated tank and the small linked system, in spite of the limited biological activity in both systems. For example, mean water-column SRP concentrations of Days 3 to 13 of Expts 1, 2 and 3 (i.e. from shortly after the nutrient spike to just before depletion: dotted symbols in Fig. 12) were, with 1.41 µmol l^{-1}, significantly higher in the isolated tank than in the linked mesocosm, with 0.69 µmol l^{-1} ($p = 0.0199$, Pillai's trace). Mean DIN water-column concentration averaged over Expts 1, 2 and 3 over the same time period (Fig. 12, dotted symbols) showed weak evidence of being enhanced in the isolated tank, with 47.75 µmol l^{-1} compared to the linked mesocosm with 36.84 µmol l^{-1} ($p = 0.0515$, Pillai's trace). Although the slopes of water-column DIN concentration over time in Expts 1, 2, and 3 were not significantly different ($p = 0.1404$), the slopes of water-column SRP concentrations over time were significantly more negative for the small linked mesocosm than the isolated tank ($p = 0.0019$). Correlations between the slopes of water-column SRP concentration over time and SRP concentration intercepts analyzed by MANOVA (Fig. 12, left bottom panel) were significantly different between the linked and isolated systems. SRP in the small linked mesocosm had steeper, more negative slopes of concentration changes over time at any given level of intercept than the isolated tank (Fig. 12 bottom left; $p = 0.0163$, Pillai's trace). We found no significant differences in the slope and intercept correlation for the DIN dynamics (Fig. 12, bottom right, $p = 0.4075$; Pillai's trace).

Variability between sequential experiments performed in different seasons (summer, fall, spring) was associated with different water-column communities and nutrient levels. For example, in Expt 3, performed in the spring, water-column DIN concentrations were more than twice as high as in Expts 1 and 2. Sediment chlorophyll *a* levels in the large systems were more than 3 times as high in Expt 3 as in Expt 2. However, despite this variability between experiments, we detected repeated significant differences over all experiments between processes in the isolated tanks and the linked mesocosms, i.e. systems that only differed in terms of benthic boundary-layer flow or were affected by system shape. The differences between the large and the small systems were dominated by light availability, to the extent that all other variability was negligible in comparison.

DISCUSSION

System shape significantly affected illumination in the water column and at the sediment interfaces, and light availability dominated the ecosystem responses in comparisons between the large and small systems.

The small systems were light-limited due to system shape, and only about 8 µE photosynthetically active radiation m^{-2} s^{-1} reached the sediment. However, the large systems, which had the same water-column height and water-surface illumination but a smaller area, were not light-limited, and about 50 µE m^{-2} s^{-1} reached the sediment. The large systems offered significantly more light to the ecosystems, resulting in higher phytoplankton biomass (25 vs 7, 100 vs 10, and 200 vs 5 µg l^{-1} chlorophyll *a* in the large vs small systems, respectively, in Expts 1, 2 and 3), and this subsequently significantly increased oyster biomass. Oysters did not grow in the small systems, but gained about 0.5 g live weight over each experiment in the large systems. Oysters were probably severely food-limited in the small systems; however, they were also likely to have been periodically food-limited in the large systems since phytoplankton concentrations were low, with about 10 mg l^{-1} chlorophyll *a* over long periods in the experiments. Oyster feeding also transported particulate organic matter to the bottom, fueling biogeochemical processes at the sediments in the large systems. In contrast, low light levels due to system shape resulted in very low overall water column activity in the small systems, less removal of phytoplankton from the water column by oysters, and less subsequent particulate organic matter deposition to the bottom, with mostly undetectable sediment nutrient fluxes. Thus, mesocosm shape is an important consideration for experimental ecosystem design. Differences in system shape can mask the results of the treatments of interest, especially if light availability is a controlling factor in those treatments. These effects can even translate to organisms, as reflected by differential oyster growth indirectly mediated by light availability. Previous studies with bivalves in mesocosms have not considered the cascading effects that lead to this food limitation or a possible effect of food limitation on the bivalves or subsequent processes (Doering et al. 1986, 1987), but some have reported food competition with dense populations (Prins et al. 1995). It should be noted that the shape of our small systems (small diameter-to-height ratio) was similar to the shape of the Marine Ecosystems Research Laboratory (MERL) mesocosms at the University of Rhode Island, and in fact similar to the most common shape used in many previous experimental ecosystem studies (review by Petersen et al. 1999). In future studies, tank designs with a small diameter-to-wall-height ratio such as the small tank design should not be used for studies that critically depend on light. The large tank design, however, did not limit light, and is a good 'practical working size', with potential for large-scale replication. Larger tank sizes than this are more difficult to work with, produce more patchiness, and cannot be replicated as often. In addition, for higher trophic levels such as fishes, Heath & Houde (2001) have shown that a diameter of no less than 1 m is the minimum size for including small fishes, though for long-term experiments with fishes 2 to 4 m diameter systems should be used.

Significant hydrodynamic effects on an indirect, biologically mediated, nutrient transport mechanism were the most dramatic result of our study. Microphytobenthos biomass significantly increased in the large systems that were not light-limited, yet even only moderately enhanced bottom shear (below sediment resuspension levels) repeatedly eroded microphytobenthos as the mat aged. In Expt 2, sediment chlorophyll *a* was, for example, reduced from 125 to about 80 mg chlorophyll *a* m^{-2}, and in Expt 3 from about 450 to 250 mg. The mass erosion events were preceded by an observed oxygen bubble formation period within the mat, also observed by Miller et al. (1996). The bubble formation may have lifted part of the microphytobenthos mat and affected mat strength and/or surface roughness, thereby effectively reducing the critical shear stress required to erode the mat. Microphytobenthos can take up nutrients or produce oxygen at the sediment–water interface and thus alter the amount of nutrients regenerated from the sediment to the water column (Sundbäck & Graneli 1988, Sundbäck et al. 1991, 2000). The presence and amount of microphytobenthos in the large systems subsequently significantly affected the direction and magnitude of biogeochemical dissolved inorganic nutrient flux exchanges between the sediments and the water column and, with this, the effective net nitrogen removal from the ecosystem. During the light phases, microphytobenthos photosynthesis induced nitrogen uptake from the water column, and during dark phases significantly less was taken up by the sediments or nitrogen was regenerated from the sediments back into the water column with potential implications for water quality. For example, dark–light DIN flux differences reached up to 320 µmol DIN m^{-2} h^{-1}. Integrated dark and light sediment fluxes showed significantly more nitrogen regeneration from the sediments to the water column in the linked mesocosm with less sediment chlorophyll *a*, i.e. 240 and 160 µmol DIN m^{-2} h^{-1} in Expts 2 and 3, respectively. Significantly less net nitrogen was removed from the ecosystem from which microphytobenthos had been eroded. Mesocosms that do not mimic benthic boundary-layer flow and bottom shear sufficient to erode microphytobenthos, as occurs typically in natural shallow environments, may overestimate microphytobenthos abundance and nitrogen removal. Moreover, microphytobenthos abundance cannot be estimated from available light alone; the physics at the sediment–water interface must be considered as well.

In typical isolated tank systems, benthic mean flow speeds are very low, and benthic shear velocity, created by the overlying water-column turbulence intensity and secondary flow (if any), is also disproportionately low; this affects diffusional mass transfers, eliminates erosion, and leads to a depositional bottom environment. In shallow coastal and estuarine environments, bottom shear is generated by currents and waves. The mass transfer velocity β of solutes or gases across the diffusive sublayer is directly proportional to shear velocity (u_*) (Opdyke et al. 1987, Dade 1993) as

$$\beta = 0.1 u_* Sc^{-0.67} = 0.1 u_* \left(\frac{\nu}{D}\right)^{-0.67} \quad (4)$$

where Sc is the Schmidt number, ν the kinematic viscosity, and D the molecular diffusion coefficient of the solute or gas. The mass transfer velocity for ammonium and soluble reactive phosphorus, for example, was about 6 times faster in the linked mesocosms than in the isolated tanks. In addition, bottom shear can affect sediment oxygenation (Booij et al. 1994) with consequences for nitrogen transformations and regeneration, and for contaminant dynamics. The isolated tanks were diffusion-limited at low water-column nutrient levels (Sanford & Crawford 2000). Enhanced diffusion may have contributed to the reduced water column SRP concentrations in the small linked system compared to the small isolated tank. It is also possible that very small particles (below our filter size of 0.8 µm) were resuspended in the linked mesocosms, adsorbing SRP onto them and leading to the observed significantly faster decrease and overall lower SRP levels in the small linked mesocosm compared to the small isolated tank.

Hydrodynamically, flows in the water column and at the sediment–water interface of shallow coastal and estuarine environments are not independent and need to be scaled correctly in experimental ecosystems. Turbulence intensity and shear velocity occur in a ratio of about 1.4:1 in nature. The design of our 2 types of linked mesocosms mimicked this ratio well with a value of 1.6:1, whereas in the isolated tanks the ratio was much too high at about 7.5:1 due to unrealistically low bottom shear velocities. Increased stirring of isolated tanks leads to higher bottom shear stress, but at the cost of unrealistically high mixing rates in the water column (Crawford & Sanford 2001). In such cases, coupling between the benthos and the water column is likely to be distorted in standard isolated tank mesocosms. The natural ratio of mean flow speed to shear velocity of about 19:1 (Table 1) is also a consideration in experimental ecosystem design. In our linked mesocosms, shear velocity was created more realistically by a mean flow across the bottom, whereas in the standard isolated tanks bottom shear was created by the overlying water-column turbulence. Mean flow speeds in the linked experimental ecosystems at about 10 cm s^{-1} greatly exceeded mean flow speeds (<2 cm s^{-1}) at the bottom of the standard isolated tank systems (Table 2). For a balanced benthic and pelagic view, as advocated by Threlkeld (1994), flow at the sediment–water interface, flow in the water column, and the relationships between them should all be considered in experimental ecosystem design.

Our results show that these hydrodynamic distortions have ecological consequences and affect the nutrient dynamics. We found that inclusion of the benthic interface with realistic bottom shear significantly affected ecosystem processes such as microphytobenthos resuspension, sediment–water nutrient exchange, and water-column nutrient dynamics. The effects were, more often than not, unanticipated, indirect, and nonlinear. Data generated from mesocosms with unrealistic flow may miss or distort such important ecosystem links. They may provide misleading results if they are scaled up to nature or are used in ecosystem models that require benthic–pelagic coupling.

Due to sequential replication, our experiments were performed at 3 different seasons with widely varying initial and exchange nutrient levels in the water column and with different initial populations. A number of variables such as water-column nutrient concentrations in the water column of the large systems were not significantly different but could have in fact been statistically significant if simultaneous replication had been used or a higher level of bottom shear. Thus, with a high experimental uncertainty level based on the variability of the biological variables, the significant results of light, oyster growth, phytoplankton abundance, sediment chlorophyll *a*, sediment DIN flux rates, and water-column SRP dynamics obtained in this study are very strong.

Our linked mesocosms had a few limitations that pertain to the way the water column and the benthic boundary-layer devices were physically connected. In these systems, we linked water columns and benthic boundary-layer devices using umbilicals equipped with automated valve systems and pumps. We chose a gentle air-lift pump design and large umbilicals in the large linked mesocosm and observed no apparent damage to copepods; however, pumping of any sort should be avoided in living ecosystems (Adey & Loveland 1998). Our current work has addressed these problems, and we have developed a mesocosm stirring design that can produce high uniform bottom shear and realistic water-column turbulence levels in a single tank. This design will be reported in a subsequent paper.

The linked experimental ecosystems developed here allow the study of benthic–pelagic coupling processes in controllable laboratory ecosystems. A wide range

of benthos and muddy sediment can be used in our linked mesocosms, and experiments with scaled levels of benthic boundary-layer flow and water-column turbulence can be performed. Sediment depth can be adjusted to accommodate deep-burrowing organisms while keeping the bottom shear at the desired levels. Plankton, contaminants, or nutrients of choice can be added for specific, scaled, and controlled experiments under natural flow and turbulence conditions. From such an approach, insights can be gained on nutrient, contaminant, and ecosystem dynamics in coastal ecosystems as mediated by biology and water flow. Scaled benthic–pelagic coupling ecosystem experiments can be designed by varying bottom shear (include sediment resuspension) and water-column turbulence levels and, for example, by varying the abundance and functional groups of the benthos to investigate a range of questions previously not possible and that include many direct and indirect linkages.

Microphytobenthos abundance has previously been found to be linearly related to light in the field and in mesocosms (e.g. MacIntyre et al. 1996, Chen et al. 1997); however, microphytobenthos abundance has also been found to correlate with shear strength and critical shear stress (Underwood & Paterson 1993). Moderate increase in shear velocity from 0.1 to 0.6 cm s^{-1} in the large linked mesocosm significantly increased microphytobenthos erosion compared to the isolated tanks, and reduced microphytobenthos biomass from about 125 to 80 mg m^{-2} and 450 to 250 mg m^{-2} in Expts 2 and 3, respectively. We observed, and in Expt 3 measured, mass erosion of microphytobenthos around Week 4 in the annular flume, a phenomenon observed previously (Miller et al. 1996), and the erosion appeared to depend on shear velocity and the age of the mat. Oxygen bubbles observed in the mat in our experiments may have lifted the carpet, increasing the roughness and leading to erosion at only moderate shear. In contrast, it has been shown that the age of the microphytobenthos mat can also reduce sediment erodability through the alteration of adhesive–cohesive bonding among particles (Madsen et al. 1993, Sutherland et al. 1998). This was not observed in our experiments. Interestingly, Blanchard et al. (2001) noted from their 11 d comparison of microphytobenthos biomass in a mesocosm setting and measurements in the intertidal zone (using relative units of microphytobenthos biomass) that microphytobenthos biomass increased in the 'physically stable' mesocosm until a biotic capacity of the environment was reached, after which biomass stayed stable, i.e. similar to our experiments in the large isolated tanks. However, they further suggested that microphytobenthos biomass in the field declined due to resuspension and grazing; yet, the variability in their field measurements was high, with chlorophyll *a* biomasses ranging from 80 to 225 mg m^{-2}. Kendrick et al. (1996) observed very different sediment chlorophyll *a* and pheopigment levels between their mesocosms and the field (Day 12: sediment chlorophyll *a* in mesocosms versus the field: 1.5 vs 0.5; pheopigments: 8 vs 2 µg mg^{-1} dry weight) and attributed the higher levels in the mesocosms to decreased water movement. Our appropriately scaled direct comparison of a standard isolated mesocosm at low bottom shear (0.1 cm s^{-1}) to a linked mesocosm at moderate bottom shear (0.6 cm s^{-1}) specifically let us address the question of an interaction of bottom shear and biology in a much more controlled manner than the approach by Kendrick et al. (1996) or Blanchard et al. (2001). The experiments in the isolated tanks with low shear velocity, an artifact of standard isolated tank mesocosms, indicated that abundant biomass can be generated when the hydrodynamics is such that the population is not eroded and entrained.

We also observed that the significant reduction in microphytobenthos biomass due to enhanced shear velocity can indirectly affect feedbacks such as nutrient regeneration from the sediments into the water column. Nutrient regeneration from the sediments may stimulate phytoplankton production (Cerco & Seitzinger 1997) and affect water quality. It has been shown that photosynthesis by microphytobenthos can reduce the rates of DIN regenerated from the sediments to the water column (Sundbäck & Graneli 1988, Sundbäck et al. 1991) or alter nutrient transformations (Sundbäck et al. 2000), and a higher-sediment DIN uptake in shallow systems may ultimately affect watercolumn DIN concentrations and water quality. However, the explanation through direct, indirect, and non-linear effects of bottom shear on these interactions has not previously been put forth.

Mean flow speed may affect ecosystem dynamics by altering the cycling of organic matter as mediated by the food supply to suspension feeders. Such flow may have resulted in a higher food supply to the oysters from resuspended microphytobenthos in our large linked system. Benthic suspension feeders such as bivalves, in interaction with water flow, can efficiently remove phytoplankton from the water column (Fréchette et al. 1989, Butman et al. 1994) and can deposit large amounts of organic matter to the sediment–water interface in their feces and pseudofeces. Above a critical shear velocity, biodeposits can be eroded and carried away from the source and thus affect the distribution of organic matter across an area (Lund 1957, Taghon et al. 1984). We observed the transport of biodeposits from oysters in the large linked mesocosm at a shear velocity of 0.6 cm s^{-1}.

The mesocosm systems developed here also permit the simulation of a variety of natural flow speeds. Such

variable mean flow speed has been found to result in some organisms such as the polychaetes *Boccardia pugettensis* and *Pseudopolydora kempi japonica* (Taghon & Greene 1992) or *Macoma balthica* (Diaz & Schaffner 1990) switching between suspension and deposit feeding. The feeding mode as affected by benthic boundary-layer flow in the mesocosms may further alter organic matter or toxic material cycling pathways and bioaccumulation and thus benthic–pelagic coupling.

Although mesocosms have been strongly criticized, the implementation of more realistic water-column turbulence and benthic boundary-layer flow in the same system resolves many of the concerns about the validity of mesocosm studies and designs voiced by Carpenter (1996, 1999) and Sanford (1997). This makes this new generation of mesocosms a promising tool for studying benthic–pelagic coupling processes in an ecosystem context that includes all the direct and indirect links so sorely missed by Threkheld (1994).

Proper mesocosm development takes time and effort. Careful attention must be given to design, construction, and physical characterization before performing ecosystem experiments. The linked experimental ecosystems developed here are a first approach towards mesocosm designs that allow realistic whole-ecosystem studies and accurately mimic benthic–pelagic coupling processes, including direct and indirect ecosystem links, processes that typical isolated tank systems fail to mimic adequately.

Acknowledgements. We thank S. Crawford for letting us use his hot-film anemometry setup, E. Perry for his help with the statistics, V. Kennedy for reading an early draft, and J. Seabrease for machining help and for teaching E.T.P. some tricks of the machining trade. Our research was supported by grant no. R 824850-01-0 from the USEPA STAR program as part of the Multiscale Experimental Ecosystem Research Center (MEERC) at the University of Maryland Center for Environmental Science (UMCES), and by a fellowship of the Horn Point Laboratory to E.T.P. This is UMCES publication no. 3700.

LITERATURE CITED

Adey WH, Loveland K (1998) Pumps. In: Adey WH, Loveland K (ed) Dynamic aquaria, building living ecosystems. Academic Press, San Diego, p 27–33

Asmus RM, Jensen MH, Jensen KM, Kristensen E, Asmus H, Wille A (1998) The role of water movement and spatial scaling for measurement of dissolved inorganic nitrogen fluxes in intertidal sediments. Estuar Coast Shelf Sci 46: 221–232

Baumert H, Radach G (1992) Hysteresis of turbulent kinetic energy in nonrotational tidal flows: a model study. J Geophys Res 97:3669–3677

Blanchard GF, Guarini JM, Orvain F, Sauriau PG (2001) Dynamic behaviour of benthic microalgal biomass in intertidal mudflats. J Exp Mar Biol Ecol 264:85–100

Bohlen W (1977) Shear stress and sediment transport in unsteady turbulent flows. Estuar Processes 2:109–124

Booij K, Sundby B, Helder W (1994) Measuring the flux of oxygen to a muddy sediment with a cylindrical microcosm. Neth J Sea Res 32:1–11

Bowden KF (1962) Measurements of turbulence near the sea bed in a tidal current. J Geophys Res 67:3181–3186

Boynton WR, Kemp WM, Osborne CG, Kaumeyer KR, Jenkins MC (1981) Influence of water circulation rate on *in situ* measurements of benthic community respiration. Mar Biol 65:185–190

Bruckner A, Kampichler C, Wright J, Bauer R, Kandeler E (1995) A method of preparing mesocosms for assessing complex biotic processes in soils. Biol Fert Soils 19: 257–262

Butman CA, Fréchette M, Geyer WR, Starczak VR (1994) Flume experiments on food supply to the blue mussel *Mytilus edulis* L. as a function of boundary-layer flow. Limnol Oceanogr 39:1755–1768

Caffrey JM, Sloth NP, Kaspar HF, Blackburn TH (1993) Effect of organic loading on nitrification and denitrification in a marine sediment microcosm. FEMS Microbiol Ecol 12: 159–167

Carpenter SR (1996) Microcosm experiments have limited relevance for community and ecosystem ecology. Ecology 77:677–680

Carpenter SR (1999) Microcosm experiments have limited relevance for community and ecosystem ecology: reply. Ecology 80:1085–1088

Cerco CF, Seitzinger SP (1997) Measured and modeled effects of benthic algae on eutrophication in Indian River–Rehoboth Bay, Delaware. Estuaries 20:231–248

Chen CC, Petersen JE, Kemp WM (1997) Spatial and temporal scaling of periphyton growth on walls of estuarine mesocosms. Mar Ecol Prog Ser 155:1–15

Chen CC, Petersen JE, Kemp WM (2000) Nutrient-uptake in experimental estuarine ecosystems: scaling and partitioning rates. Mar Ecol Prog Ser 200:103–116

Crawford SM, Sanford LP (2001) Boundary shear velocities and fluxes in the MEERC experimental ecosystems. Mar Ecol Prog Ser 210:1–12

Dade WB (1993) Near-bed turbulence and hydrodynamic control of diffusional mass transfer at the sea floor. Limnol Oceanogr 38:52–69

Dame R, Libes S (1993) Oyster reefs and nutrient retention in tidal creeks. J Exp Mar Biol Ecol 171:251–258

Deardorff JW, Yoon SC (1984) On the use of an annulus to study mixed layer entrainment. J Fluid Mech 142:97–120

de Wilde PAWJ (1990) Benthic mesocosms. I. Basic research in soft-bottom benthic mesocosms. In: Lalli CM (ed) Enclosed experimental marine ecosystems: a review and recommendations, Springer-Verlag, New York, p 109–121

Diaz RJ, Schaffner LC (1990) The functional role of estuarine benthos. In: Haire M, Krome EL (eds) Perspectives on the Chesapeake Bay, 1990: advances in estuarine science. United States Environmental Protection Agency for the Chesapeake Bay Program, Baltimore, p 25–56

Doering PH, Oviatt CA, Kelly JF (1986) The effects of the filter feeding clam *Mercenaria mercenaria* on carbon cycling in experimental mesocosms. J Mar Res 44:839–861

Doering PH, Kelly JR, Oviatt CA, Sowers T (1987) Effect of the hard clam *Mercenaria mercenaria* on benthic fluxes of inorganic nutrients and gases. Mar Biol 94:377–383

Duarte CM, Gasol JM, Vaque D (1997) Role of experimental approaches in marine microbial ecology. Aquat Microb Ecol 13:101–111

Fingerson LM, Freymuth P (1983) Thermal anemometers. In:

Goldstein RJ (ed) Fluid mechanics measurements, 2nd edn. Taylor & Francis, Washington, DC, p 99–153

Fréchette M, Butman CA, Geyer WR (1989) The importance of boundary-layer flows in supplying phytoplankton to the benthic suspension feeder, *Mytilus edulis* L. Limnol Oceanogr 34:19–36

Gordon C, Dohne C (1973) Some observations of turbulent flow in a tidal estuary. J Geophys Res 78:1971–1978

Gross T, Nowell A (1983) Mean flow and turbulence scaling in a tidal boundary layer. Contin Shelf Res 2:109–126

Gust G (1988) Skin friction probes for field applications. J Geophys Res 93:14 121–14 132

Gust G, Müller V (1997) Interfacial hydrodynamics and entrainment functions of currently used erosion devices. In: Burt N, Parker R, Watts J (eds) Cohesive sediments. John Wiley & Sons, New York, p 149–174

Haag D, Matschonat G (2001) Limitations of controlled experimental systems as models for natural systems: a conceptual assessment of experimental practices in biogeochemistry and soil science. Sci Total Environ 277:199–216

Heath MR, Houde ED (2001) Evaluating and modeling foraging performance of planktivorous and piscivorous fish. Effect of containment and issues of scale. In: Gardner RH, Kemp WM, Kennedy VS, Petersen JE (eds) Scaling relations in experimental ecology. Columbia University Press, New York, p 191–122

Henriksen K, Kemp WM (1988) Nitrification in estuarine and coastal marine sediments: methods, patterns and regulating factors. In: Blackburn H, Sørensen J (eds) Nitrogen cycling in coastal marine environments. John Wiley & Sons, New York, p 207–250

Jensen MH, Lomstein E, Sorensen J (1990) Benthic NH_4^+ and NO_3^- flux following sedimentation of a spring phytoplankton bloom in Aarhus Bight, Denmark. Mar Ecol Prog Ser 61:87–96

Kampichler C, Bruckner A, Kandeler E (2001) Use of enclosed model ecosystems in soil ecology: a bias towards laboratory research. Soil Biol Biochem 33:269–275

Kendrick GA, Jacoby CA, Heinemann D (1996) Benthic microalgae: comparisons of chlorophyll *a* in mesocosms and field sites. Hydrobiologia 327:283–289

Lorenzen CJ (1967) Determination of chlorophyll and phaeopigments: spectrophotometric equations. Limnol Oceanogr 12:343–346

Ludwieg H, Tillman W (1949) Untersuchung über die Wandschubspannung in turbulenten Reibungsschichten. Ing-Arch 17:288–299

Lund EJ (1957) Self silting, survival of the oyster as a closed system, and reducing tendencies of the environment of the oyster. Publ Inst Mar Sci Univ Tex 4:313–319

Maa JPY, Wright LD, Lee CH, Shannon TW (1993) VIMS sea carousel: field instrument for studying sediment transport. Mar Geol 115:271–287

MacIntyre HL, Geider RJ, Miller DC (1996) Microphytobenthos: the ecological role of the 'Secret Garden' of unvegetated, shallow-water marine habitats. I. Distribution, abundance and primary production. Estuaries 19:186–201

Madsen KN, Nilsson P, Sundbäck K (1993) The influence of benthic microalgae on the stability of a subtidal sediment. J Exp Mar Biol Ecol 170:159–177

Mann KH, Lazier JRN (1991) Biology and boundary layers. In: Mann KH, Lazier JRN (eds) Dynamics of marine ecosystems, biological-physical interactions in the oceans. Blackwell, Oxford, p 9–60

Miller DC, Geider RJ, Macintyre HL (1996) Microphytobenthos: the ecological role of the 'Secret Garden' of unvegetated, shallow-water marine habitats. II. Role in sediment stability and shallow-water food webs. Estuaries 19: 202–212

Muschenheim DK, Grant J, Mills EL (1986) Flumes for benthic ecologists: theory, construction and practice. Mar Ecol Prog Ser 28:185–198

Nowell ARM, Jumars PA (1984) Flow environments of aquatic benthos. Annu Rev Ecol Syst 15:303–328

Opdyke BN, Gust G, Ledwell JR (1987) Mass transfer from smooth alabaster surfaces in turbulent flow. Geophys Res Lett 14:1131–1134

Parsons TR, Takahashi M, Hargrave B (1984) Biological oceanographic processes. Pergamon, Oxford

Perez KT, Morrison GM, Lackie NF, Oviatt CA, Nixon SW, Buckley BA, Heltshe JF (1977) The importance of physical and biotic scaling to the experimental simulation of a coastal marine ecosystem. Helgol Wiss Meeresunters 30: 144–162

Petersen JE, Cornwell JC, Kemp WM (1999) Implicit scaling in the design of experimental aquatic ecosystems. Oikos 85:3–18

Porter ET (1999) Physical and biological scaling of benthic–pelagic coupling in experimental ecosystem studies. PhD thesis, University of Maryland, College Park

Porter ET, Sanford LP, Suttles SE (2000) Gypsum dissolution is not a universal integrator of 'water motion'. Limnol Oceanogr 45:145–158

Porter ET, Cornwell JC, Sanford LP (2004) Effects of oysters *Crassostrea virginica* and bottom shear velocity on benthic–pelagic coupling and estuarine water quality. Mar Ecol Prog Ser 271:61–75

Prins TC, Escaravage V, Smaal AC, Peeters, JC (1995) Nutrient cycling and phytoplankton dynamics in relation to mussel grazing in a mesocosm experiment. Ophelia 41: 289–315

Prins TC, Escaravage V, Pouwer AJ, Wetsteyn LPMJ, Haas HA (1997) Description of mesocosms and methods, and a comparison with North Sea conditions. In: Smaal AC, Peeters JCH, Prins TC, Haas HA, Heip CHR (eds) The impact of marine eutrophication on phytoplankton, zooplankton and benthic suspension feeders. Report RIKZ-97.035, NIOO/CEMO-1997.05. National Institute for Coastal and Marine Management, Middelburg, p 19–40

Sanford LP (1997) Turbulent mixing in experimental ecosystem studies. Mar Ecol Prog Ser 161:265–293

Sanford LP, Crawford SM (2000) Mass transfer versus kinetic control of uptake across solid-water boundaries. Limnol Oceanogr 45:1180–1186

Santschi P, Hohener P, Benoit G, Brink MBT (1990) Chemical processes at the sediment–water interface. Mar Chem 30: 269–315

Schindler DW (1998) Replication versus realism: the need for ecosystem-scale experiments. Ecosystems 1:323–334

Sebens KP (1994) Biodiversity of coral-reefs—what are we losing and why. Am Zool 34:115–133

Sheng YP (1989) Consideration of flow in rotating annuli for sediment erosion and deposition studies. J Coast Res 51: 207–216

Steel RGD, Torrie JH (1980) Principles and procedures of statistics, a biometrical approach, 2nd edn. MacGraw-Hill, New York

Sullivan BK, Doering PH, Oviatt CA, Keller AA, Frithsen JB (1991) Interactions with the benthos alter pelagic food web structure in coastal waters. Can J Fish Aquat Sci 48: 2276–2284

Sundbäck K, Graneli W (1988) Influence of microphytobenthos on the nutrient flux between sediment and water—a laboratory study. Mar Ecol Prog Ser 43:63–69

Sundbäck K, Enoksson V, Graneli W, Pettersson K (1991) Influence of sublittoral microphytobenthos on the oxygen and nutrient flux between sediment and water—a laboratory continuous-flow study. Mar Ecol Prog Ser 74:263–279

Sundbäck K, Miles A, Goransson E (2000) Nitrogen fluxes, denitrification and the role of microphytobenthos in microtidal shallow-water sediments: an annual study. Mar Ecol Prog Ser 200:59–76

Sutherland TF, Grant J, Amos CL (1998) The effect of carbohydrate production by the diatom *Nitzschia curvilineata* on the erodibility of sediment. Limnol Oceanogr 43: 65–72

Taghon GL, Greene RR (1992) Utilization of deposited and suspended particulate matter by benthic 'interface' feeders. Limnol Oceanogr 37:1370–1391

Taghon GL, Nowell ARN, Jumars PA (1984) Transport and breakdown of fecal pellets: biological and sedimentological consequences. Limnol Oceanogr 29:64–72

Tennekes H, Lumley JL (1972) A first course in turbulence, 15th edn. MIT Press, Cambridge, MA

Tenore K, Boyer L, Cal R, Corral J and 14 others (1982) Coastal upwelling in the Rhias of NW Spain: contrasting the benthic regime of the Rhias de Arosa and de Mu. J Mar Res 40:701–768

Terray EA, Donelan MA, Agrawal YC, Drennan WM, Kahma KK, Williams AJ III, Hwang PA, Kitaigorodskii SA (1996) Estimates of energy dissipation under breaking waves. J Phys Oceanogr 26:792–807

Thomsen L, Flach E (1997) Mesocosm observations of fluxes of particulate matter within the benthic boundary layer. J Sea Res 37:67–79

Threkheld S (1994) Benthic–pelagic interactions in shallow water columns: an experimentalist's perspective. Hydrobiologia 275/276:293–300

Underwood GJC, Paterson DM (1993) Seasonal changes in diatom biomass, sediment stability and biogenic stabilization in the Severn Estuary. J Mar Biol Assoc UK 73: 871–887

Vallino JJ (2000) Improving marine ecosystem models: use of data assimilation and mesocosm experiments. J Mar Res 58:117–164

Van Heukelem L, Lewitus AJ, Kana TM, Craft NE (1992) High-performance liquid-chromatography of phytoplankton pigments using a polymeric reversed-phase C-18 column. J Phycol 28:867–872

Van Heukelem L, Lewitus J, Kana TM, Craft NE (1994) Improved separations of phytoplankton pigments using temperature-controlled high-performance liquid-chromatography. Mar Ecol Prog Ser 114:303–313

Watts MC, Bigg GR (2001) Modelling and the monitoring of mesocosm experiments: two case studies. J Plankton Res 23:1081–1093

Editorial responsibility: Otto Kinne (Editor), Oldendorf/Luhe, Germany

Submitted: January 24, 2003; Accepted: November 18, 2003
Proofs received from author(s): April 15, 2004